DEEP INELASTIC SCATTERING OF MUONS

G. SMADJA

Département de Physique des Particules Elémentaires
Centre d'Etudes Nucléaires de Saclay
91191 Gif-sur-Yvette, France

I. INTRODUCTION

From 1970 to 1979, extensive measurements of eH_2 and eD_2 deep inelastic scattering have been performed at the Stanford accelerator, covering the range $0.1 < x < 0.9$; $1 < Q^2$ 20 GeV^2 [1], [2].

We report on recent results from two experiments on muon deep inelastic scattering at the CERN SPS, obtained with carbon targets by the BCDMS Collaboration [3], with iron, hydrogen and deuterium targets by the European muon collaboration [4].

The energy of the muon beam varies from 120 to 280 GeV, and the accessible Q^2 range extends up to 200 GeV^2, ten times more than could be reached at the Stanford Linear Accelerator.

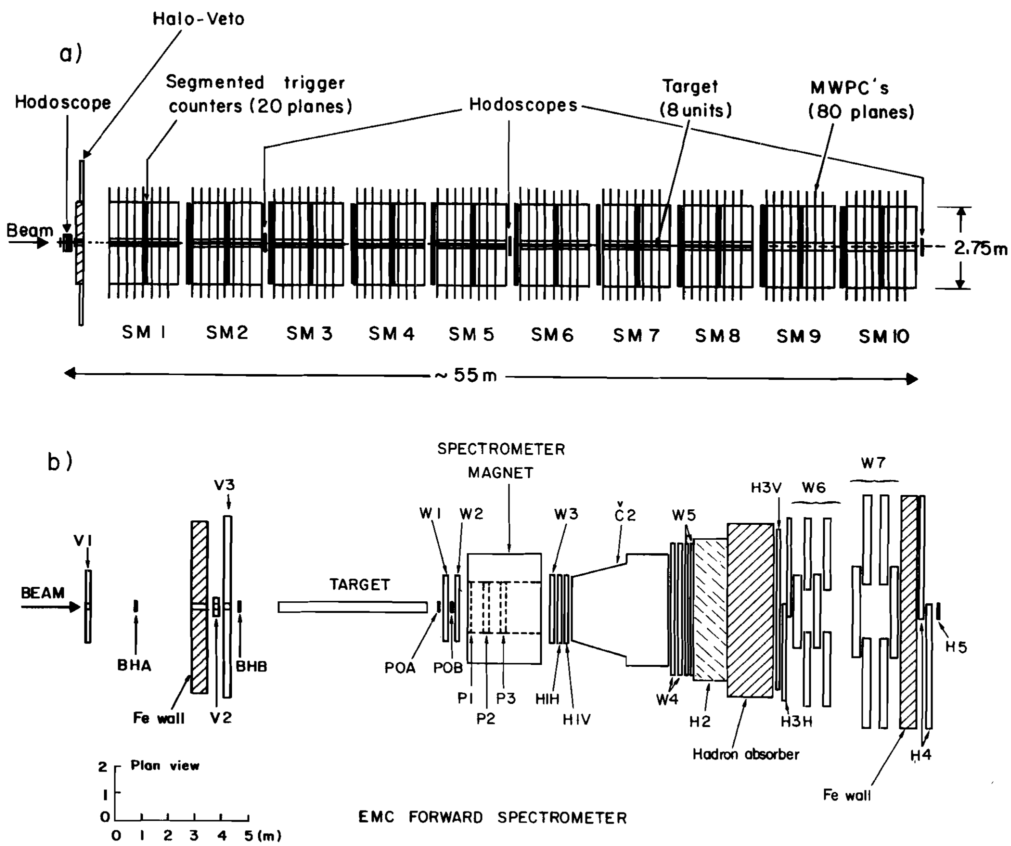

Fig. 1 - a) The BCDMS lay out. b) The EMC lay out.

The BCDMS apparatus is specifically designed for high Q^2 study, and consists of a 40 m carbon target surrounded by toroids of magnetised iron. The muon beam is defined by a set of beam hodoscopes shown in figure 1a.

On the other hand, the EMC spectrometer (Fig. 1b) is built around an air core magnet which measures the momentum of the scattered muon with an excellent accuracy : $\frac{\Delta p}{p} = 10^{-5}\ p_{GeV}$ instead of $\Delta p/p \simeq 7$ % with the iron toroids. Two sets of beam hodoscopes allow an analysis of the beam phase space, and the acceptance of this set up is good down to scattering angles of 7 mr. More details on this apparatus are given in [5].

The kinematical domain of recent e and μ scattering experiments [6] are shown on figure 2. The two CERN experiments are limited at x > 0.7 by statistics (EMC) or smearing corrections which would exceed 40 % (BCDMS).

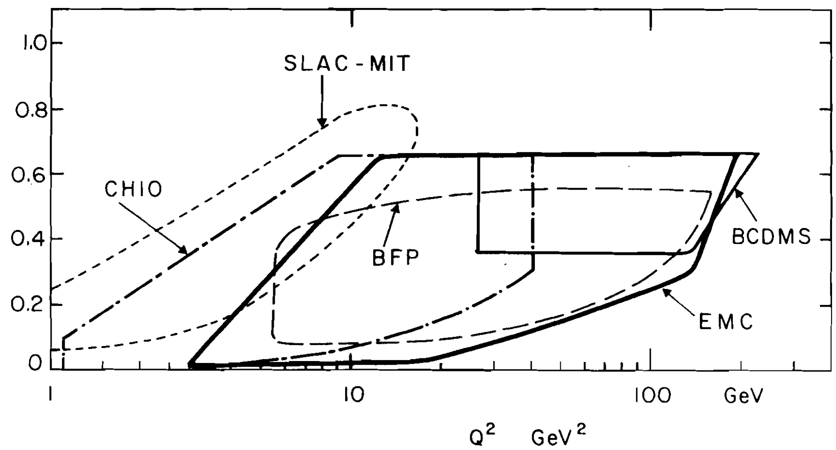

Fig. 2 - Acceptance domain of recent experiments given in ref. [6].

II. SYSTEMATICS

1°) Calibrations

A major difficulty in the measurement of structure function is the sensitivity to calibration errors. It is seen in figure 3a) that a 1 % systematic shift in the momentum determination of the beam or scattered muon can generate effects mimicking scaling violations of 10 % at x > 0.5. Great care was therefore taken to check the beam line and the spectrometers.

The stability of the beam magnets was controlled by hall probes to within 3.10^{-4}. Furthermore, the momentum of beam particles was measured in each spectrometer, and compared to the nominal setting with the following conclusions.

For EMC : $\frac{\Delta p}{p} = \frac{p_{nom} - p_{spect}}{p} = -3.10^{-3} \pm 3.10^{-3}$ at 120, 200, 280 GeV.

For BCDMS : $\frac{\Delta p}{p} = -5.10^{-3} \pm 5.10^{-3}$ at 120 GeV.

The magnetic field integrals were remeasured and found correct to within 2.10^{-3}, leaving us with a 3.10^{-3} uncertainty on the absolute calibration of the beam line.

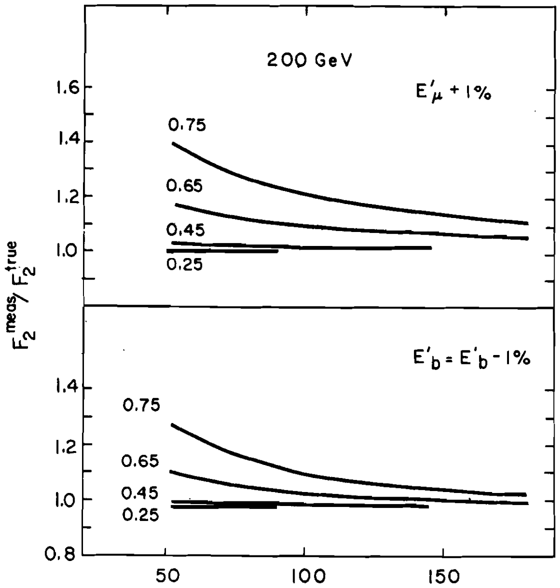

Fig. 3a) - Effect of a 1 % calibration error on the beam (Eb) or spectrometer (Eμ).

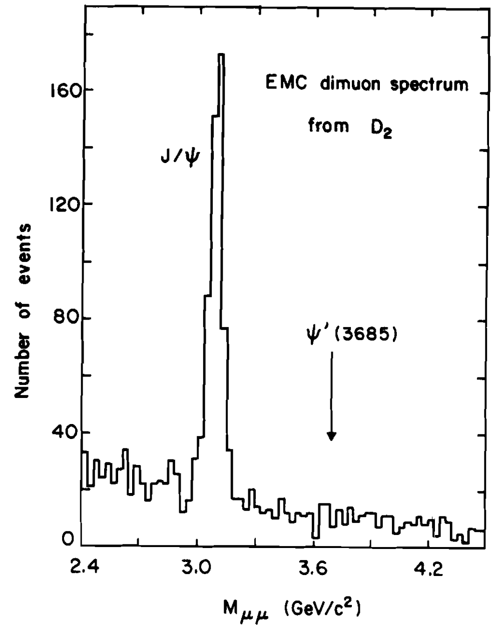

Fig. 3b) - ψ signal from the EMC experiment in μD_2 scattering.

The ψ signal of figure 3b) observed by the EMC collaboration in μD_2 scattering allows a cross check of their spectrometer : $M(\psi) = 3.082 \pm 0.007$ GeV, implying that the absolute calibration is good to 4.10^{-3}.

Finally, the energy loss in iron was rederived, remeasured by the BCDMS collaboration, and found to agree with the tables of Serre [7] to within 2 % at 100 GeV.

2°) Beam

The natural spread of the beam momentum is $\Delta p/p \sim 4$ %, but each beam particle is measured by beam hodoscopes to an accuracy of 3.10^{-3}. The phase space of the beam is monitored by 2 sets of beam hodoscopes, 6 m apart in the EMC detector. The granularity of 6 mm defines the mean divergence to an accuracy of 0.2 mr.

3°) Corrections for other physical effects

We restrict ourselves to three items :

i) Radiative corrections reach 20 % at $Q^2 \sim 20$ GeV^2 for $x < 0.1$. The elastic tail computed by Mo and Tsai [8], Akhundov et al. [9] agrees with a measurement of single photon emission by elastic events ($E_H < 0.2$ x) performed by the EMC collaboration [10] and shown on figure 4. No extra correction for multiphoton emission, as derived by Chahine [11] seems to be needed in this x range. Note that only the elastic tail of μp scattering is thus experimentally checked at this stage.

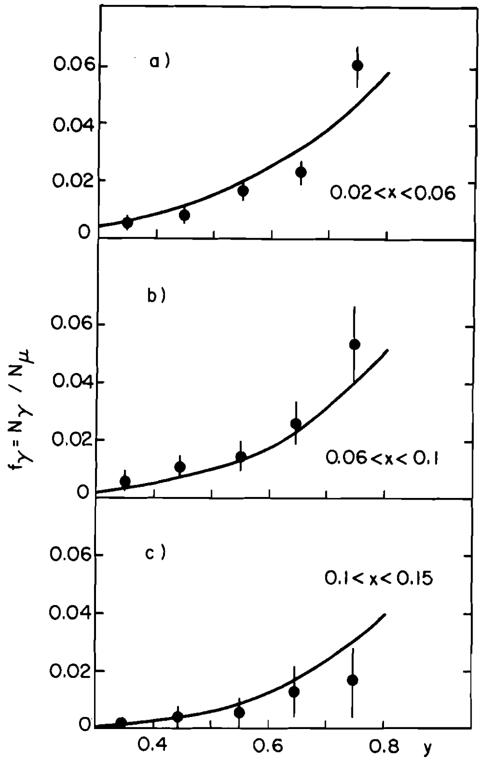

Fig. 4 - Rate of single γ emission by Bremsstrahlung measured by EMC.

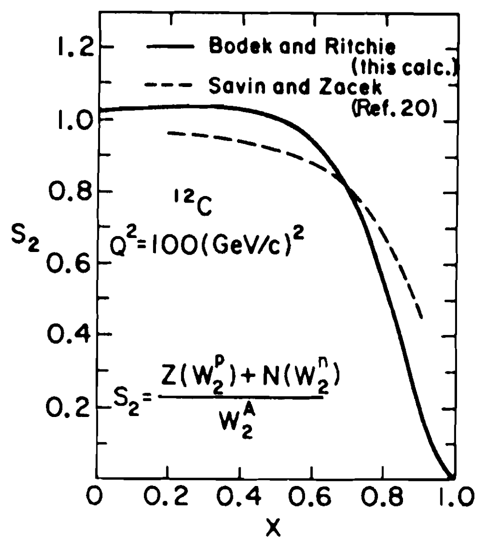

Fig. 5 - Fermi motion correction factor as a function of x. Full line from ref. [13] Dotted line from ref. [12].

ii) Fermi motion

No Fermi motion corrections were applied to the determination of the F_2 functions presented here. There are ambiguities in the recipes which should be used concerning :

- The momentum distribution inside the nucleus.
- The treatment of the binding energy of the target nucleon ($E = \sqrt{p^2 + M^2}$ in the model of Savin and Zacek [12], without correction from the binding potential.
- The kinematics of the process, described by an interaction on a D_2 pair at rest by Bodek and Ritchie [13].

Evidence will be presented pointing to the necessity of these Fermi motion corrections shown on figure 5 for $Q^2 = 10$ GeV^2.

iii) Charm production

Threshold effects from charm production should be separated from logarithmic scaling violations. The charm contribution was however measured by Clark et al. [14] and does not exceed 3 % at $x < 0.2$. They were not subtracted from the data and do not affect the measurement of scaling violations, which is done at $x > 0.25$.

III. CROSS SECTIONS AND F_2 MEASUREMENTS

The deep inelastic cross section

$$\frac{d\sigma}{dQ^2dx} = \frac{4\pi\alpha^2}{(Q^2)^2}\frac{F_2}{x}\left[1 - y + \frac{Q^2}{4E^2(1+R)}\left(1 - R + \frac{Q^2}{2M^2x^2}\right)\right]$$

depends upon two functions $F_2(x, Q^2)$, $R(x, Q^2)$ where according to the standard notations :

- Q^2 is the four momentum transfer
- ν the virtual photon energy
- $y = \nu/E$
- $x = Q^2/2M\nu$.
- R is the ratio of longitudinal and transverse cross sections for virtual photons.

It is known that $R \to 0$ as $Q^2 \to 0$, and the Callan Gross [15] relation for spin 1/2 partons implies $R \to 0$ as $Q^2 \to \infty$.

The value $R = 0$ was assumed in the F_2 measurement presented by the EMC and BCDMS collaborations. Preliminary results on R, obtained by comparing differential cross sections at the same values of x, Q^2 at different energies are reported :

(BCDMS)	$R = 0 \pm 0.2$	$x > 0.3$	$Q^2 > 30$ GeV^2
(EMC - H_2)	$R = 0.03 \pm 0.1$	$x > 0.03$	$Q^2 > 2.0$ GeV^2
(EMC - Fe)	$R = -0.13 \pm 0.2$	$x > 0.05$	$Q^2 > 3$ GeV^2

i) F_2 measurements on "isoscalar" target

The function $F_2(x, Q^2)$ is obtained in μ scattering on iron by the EMC collaboration in the range $0.03 < x < 0.7$. As seen on figure 6, the upper Q^2 range is obtained from the high energy data at 250/280 GeV.

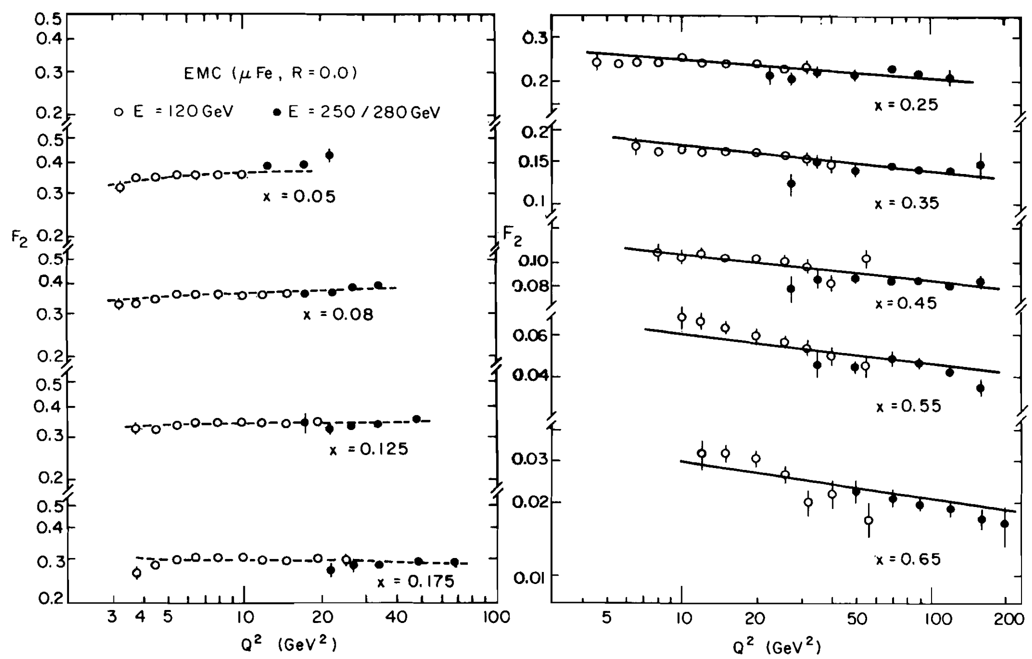

Fig. 6 – F_2 from μFe scattering by EMC at 120 and 250/280 GeV.

Comparable data from the BCDMS collaboration give the muon carbon scattering at 120, 200, 280 GeV/c in the restricted range $0.2 < x < 0.07$. It is clear that some systematic discrepancies are showing up on figure 7a) in bin $x = 0.65$.

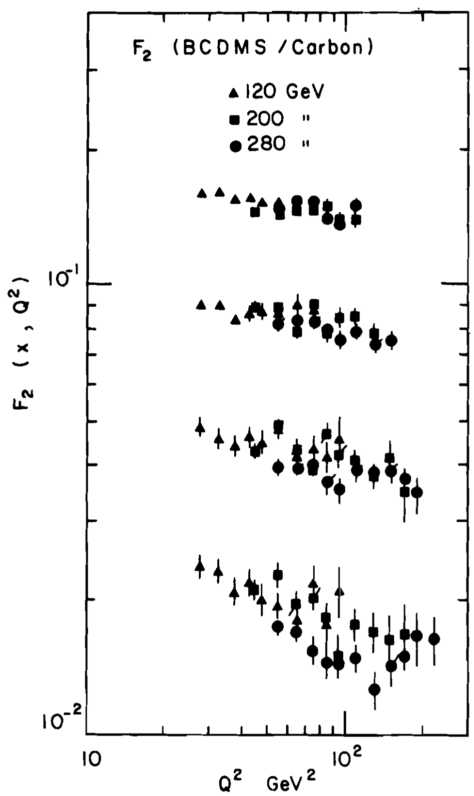

Fig. 7a) – F_2 from μC scattering by BCDMS at 120, 200, 250 GeV.

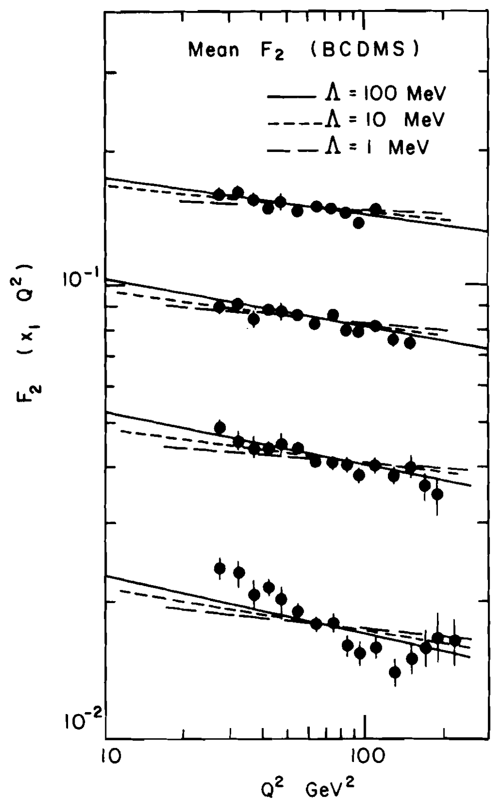

Fig. 7b) – Mean F_2 from μC scattering by BCDMS. Best Altarelli Parisi fits with Λ = 1 (– –), 10 (---), 100 MeV (——) are shown.

These systematics tend to be partially smoothed out when one averages F_2 over several energies, as in figure 7b) : the sensitive low Q^2 regions moving with E_{beam}.

The EMC data points are compared on figure 8 to a smooth fit to the BCDMS F_2 functions, and the ratio $r = F_2(EMC)/F_2(BCDMS)$ is shown as a function of x and Q^2. Figure 8 suggests some disagreement at $x = 0.65$, where r is about 1.15. Once Fermi corrections from Bodek [13] are properly included, the discrepancy becomes however smaller. A comparison with the F_2 structure functions from neutrino scattering on iron, as measured by CDHS [16], is given on figure 9. The ratio is compatible with 1 within statistical fluctuations at $x \geqslant 0.35$. There is a small discrepancy of the order of 5 to 10 % at low x, where the μ structure function lies above $5/18\ F_2^{\nu}$.

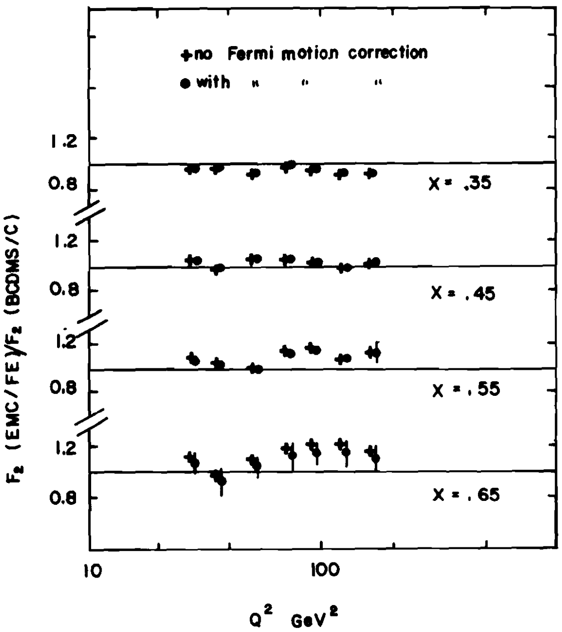

Fig. 8 - Ratio between $F_2^{\mu C}$ (BCDMS) and $F_2^{\mu Fe}$(EMC) as a function of x and Q^2, with (o) and without (O) Fermi motion correction.

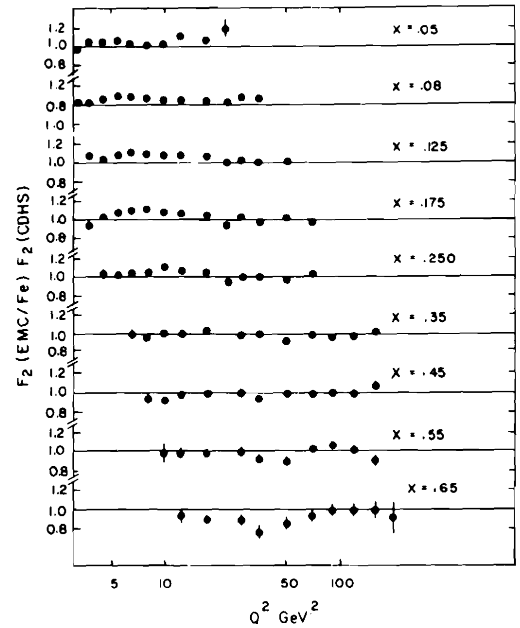

Fig. 9 - Ratio of $F_2^{\mu Fe}$ (EMC) to $F_2^{\nu Fe}$ (CDHS) as a function of (x, Q^2).

On a target with the same number of neutrons and protons :

$$F_2^{\mu} = \frac{5}{18}\,(u + \bar{u} + d + \bar{d}) + \frac{4}{9}\,(c + \bar{c}) + \frac{1}{9}\,(s + \bar{s})$$

$$F_2^{\nu} = u + \bar{u} + d + \bar{d} + 2(s + \bar{c})$$

$$F_2^{\mu} - \frac{5}{18}\,F_2^{\nu} = (\frac{4}{9}\,c - \frac{1}{9}\,\bar{c}) - (\frac{4}{9}\,s - \frac{1}{9}\,\bar{s})$$

one would naively expect $c(x) = \bar{c}(x)$; $s(x) = \bar{s}(x)$ although this is not necessarily true locally. Then :

$$F_2^{\mu} - \frac{5}{18}\,F_2^{\nu} = \frac{1}{3}\,(c - s)$$

A positive sign implies $c > s$, which is slightly unexpected. The result is more probably due to systematic uncertainties.

Once we have gained confidence in the quality of the data from scattering on heavy targets, we turn to a comparison with eD_2 from [2]. The overlapping region for μ (EMC) and e (SLAC-MIT) measurements is restricted to one or two Q^2 bins varying from 6 GeV^2 as x grows to 0.65. The ratio $r_1 = F_2(\mathrm{EMC,Fe})/F_2(\mathrm{SLAC\text{-}MIT},D_2)$ is given on figure 10a) as a function of x, and is seen to decrease from 1 to 0.8.

This is unlikely to be due to a measurement error from the EMC data, given the remarkable agreement between the two muon experiments, and between CDHS [16] and EMC data. Moreover, the preliminary result of EMC on σ_n/σ_p, discussed later on, can be used to estimate $r_2 = F_2 \text{ (EMC - Fe)} / F_2 \text{(EMC - } D_2)$ assuming

$$r_2 = \frac{\text{(Fe - EMC)}}{(\text{H2 - EMC})} \times \frac{2}{1 + \sigma_n/\sigma_p}$$

. The trend, shown on figure 10b) is the same so that the change of r_1 as a function of x does not arise from systematics in the SLAC-MIT data. The most likely conclusion is that the cause is some physical effect linked to heavy targets.

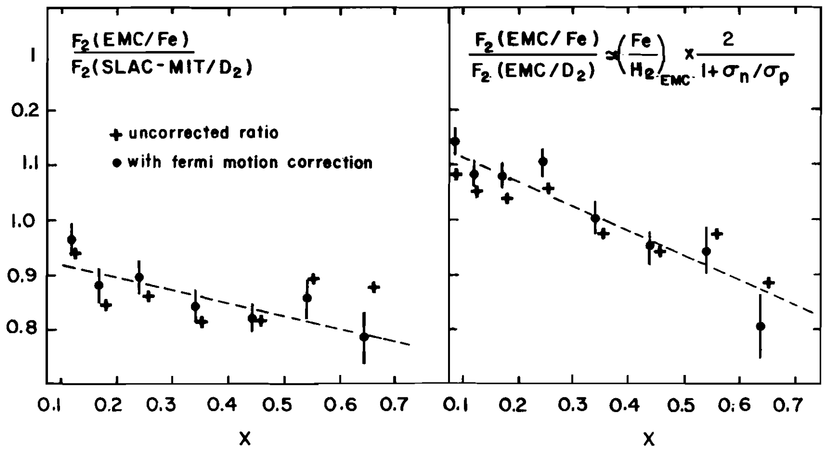

Fig. 10a) - Ratio of $F_2^{\mu Fe}$ (EMC) to F_2^{eD2} (SLAC-MIT) [2].

Fig. 10b) - Ratio of $F_2^{\mu Fe}$ (EMC) to $F_2^{\mu D2}$ (EMC).

ii) F_2 measurement on H_2

The EMC collaboration has measured F_2 in deep inelastic scattering on H_2 at 120 and 280 GeV. Figure 11 shows that the two sets of F_2 values are in excellent agreement up to X = 0.45. The statistical errors become larger beyond this value.

The comparison of μp and ep scattering on figure 12 shows no x dependence, but a 10 % overall discrepancy. We note that the same 10 % off set could be observed when comparing figure 10a) and figure 10b) : it is at the edge of the difference allowed be systematic uncertainties on normalisation (5 % for [2], 3 % for EMC) and might be partially due to the different values used for $R = \sigma_L/\sigma_T$ in extracting F_2. R is measured to be 0 ± 0.1 by EMC ($Q^2 > 10$ GeV^2), while it was found to be 0.137 in [2] ($Q^2 < 10$ GeV^2).

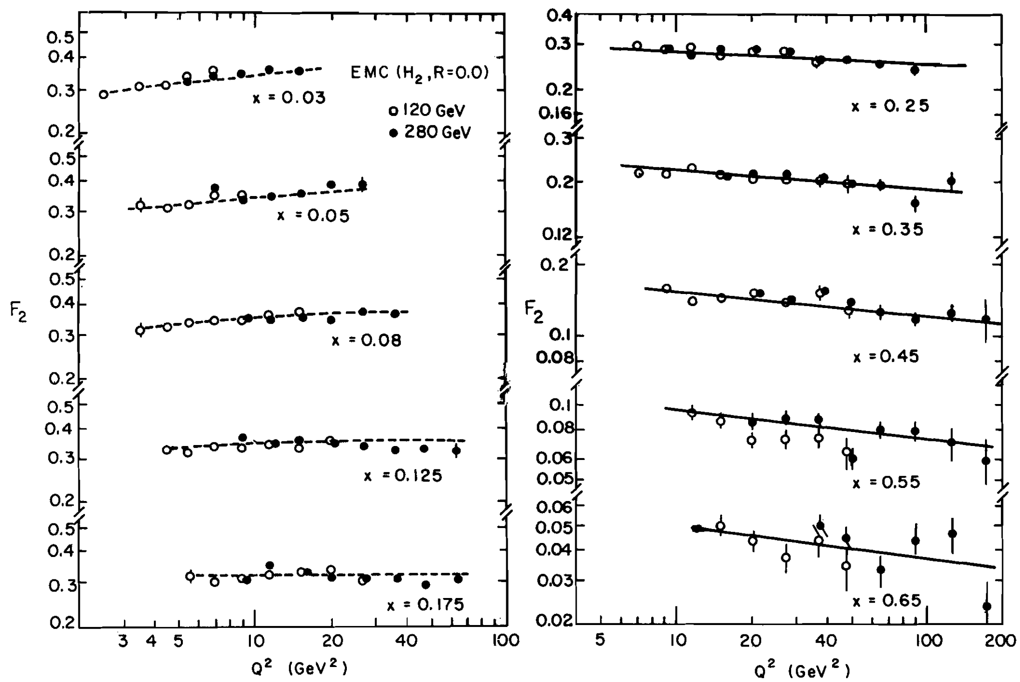

Fig. 11 - F_2 from μH_2 scattering by EMC.

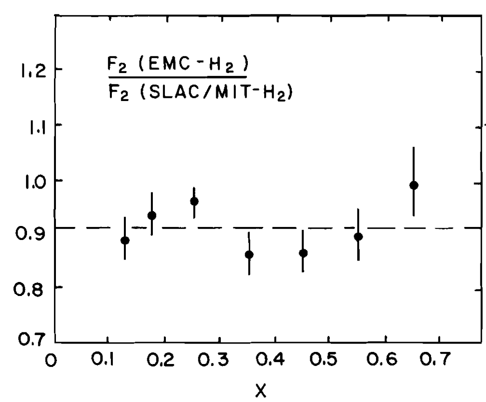

Fig. 12 - Ratio of $F_2^{\mu H2}$ (EMC) to F_2^{eH2} (SLAC-MIT) [2].

IV. ANALYSIS OF SCALING VIOLATIONS

i) Evolution equations

Most recent attempts to extract the scale violation parameter Λ make use of computer programs written by Abbot, Atwood and Barnett [17], Lopez, Yndurain and Gonzales-Arroyo [18], which solve the Altarelli, Parisi evolution equations [19] :

$$\frac{dq}{d\,\mathrm{Log}\,Q^2} = \frac{\alpha_S(Q^2)}{2\pi} \int_x^1 \frac{dy}{y} \left\{ q(y,\,Q^2)\, P_{qq}(\tfrac{x}{y}) + G(x,\,Q^2)\, P_{qg}(\tfrac{x}{y}) \right\} \tag{2}$$

$$\frac{dq}{d\,\mathrm{Log}\,Q^2} = \frac{\alpha_S(Q^2)}{2\pi} \int_x^1 \frac{dy}{y} \left\{ \sum_i q_i(y,\,Q^2)\, P_{gq}(\tfrac{x}{y}) + G(x,\,Q^2)\, P_{gg}(\tfrac{x}{y}) \right\} \tag{3}$$

F_2 obeys the same equation as xq

$$\frac{d\,F_2}{d\,\mathrm{Log}\,Q^2} = \frac{\alpha_S(Q^2)}{2\pi} \int_x^1 dz \left\{ F_2(\tfrac{x}{z},\,Q^2)\, P_{qq}(z) + 2\,N_f\, G(\tfrac{x}{z},\,Q^2)\, P_{gq}(z) \right\} \tag{4}$$

$\alpha_S(Q^2) = \dfrac{12\pi}{(33 - 2\,N_f)\,\mathrm{Log}\,\frac{Q^2}{\Lambda^2}}$ is the strong coupling constant where N_f is usually chosen to be 4 the number of "active" flavours in the hadronic mass range considered. At some value $Q^2 = Q_0^2$ (Q_0^2 varying between 5 and 20 GeV^2 depending upon the experiments) an input parametrisation of F_2 is assumed :
$F_2(x,\,Q_0^2) = Ax^{\alpha}(1-x)^{\beta}\,(1-\gamma x)$. A last unknown ingredient in equations (3), (4) is the gluon distribution $G(x,\,Q_0^2)$ which is supposed to be zero (for $x > 0.3$) or to follow a power law $(1-x)^n$, with n = 3, 5 or 7. The latest value n = 7 is in accordance to naive counting rules [20] but cannot be valid at all Q^2 since G obeys (3).

ii) Large x analysis

If x is large enough ($x > 0.3$), one can assume $G(x) = 0$, as justified by the CDHS [16] determination of G. Equation (4) takes the simplified form

$$\frac{d\,F_2}{d\,\mathrm{Log}\,Q^2} = \frac{\alpha_S(Q^2)}{2} \int_x^1 dz\, F_2(\tfrac{x}{z},\,Q^2)\, P_{qq}(z) \tag{5}$$

identical to the evolution equation for "non singlet" expressions such us $q - \bar{q}$ or $F_2^{\mu p} - F_2^{\mu n}$ (although F_2 is a pure singlet for scattering on an isoscalar target). The programs can then fit A, α, β, γ, Λ to the F_2 data points. The results for Λ are as follows :

		Λ (MeV)	Stat.	Syst.	χ^2/N
BCDMS	120 + 200 $x > 0.3$	85	+60 −40	+90 −70	1.6
BCDMS	120 + 200 + 280 $x > 0.3$	10	+10 − 6	+50 − 9	1.6
EMC-H_2	120 + 280 $x \geqslant 0.25$	110	+58 −46	+124 −69	1.45
EMC-Fe	120 + 250 + 280 $x \geqslant 0.25$	122	+22 −20	+114 −40	2.1

The systematical error is mostly due to calibration and normalisation uncertainties. Figures 7b, 13 show the best fits for Λ = 1, 10, 100 MeV to the BCDMS and EMC data, and give some insight into the sensitivity of these determinations.

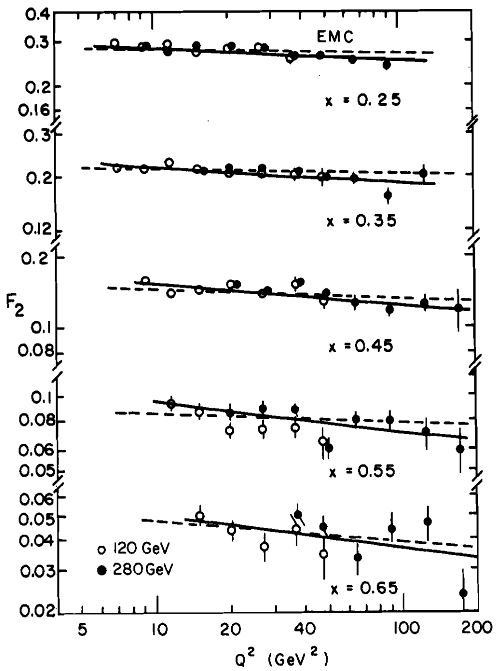

Fig. 13 - Comparison of $F_2^{\mu H_2}$ (EMC) with 2 QCD fits. Λ = 10 MeV (dotted) and Λ = 100 MeV (continuous line).

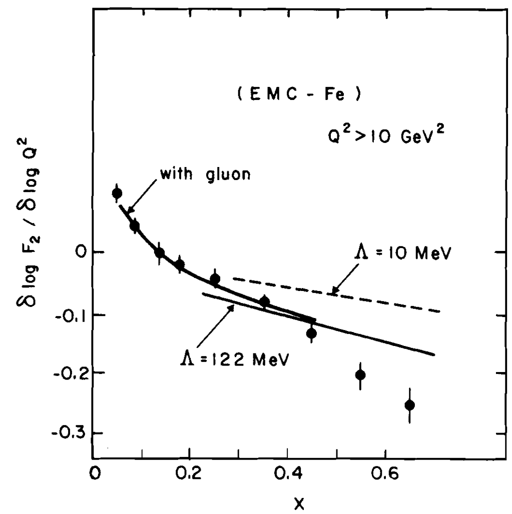

Fig. 14 - Logarithmic slopes of $F_2^{\mu Fe}$ (EMC) : $\delta \log F_2/\delta \log Q^2$ as a function of x for $Q^2 > 4$ GeV^2.

The logarithmic slopes $\partial \mathrm{Log}\, F_2/\partial \mathrm{Log}\, Q^2$ emphasize the scale breaking behaviour of the data. Furthermore, these slopes are equal to the anomalous exponents in Q^2 which characterize scaling violations. It is easily seen on figure 14 that the EMC-Fe data is not compatible with Λ = 10 MeV, although this was not apparent on figure 13.

Uncertainties on normalisation and calibration do not alter this statement.

On the other hand, the error bars on the slopes of the BCDMS carbon data on figure 15 are larger, as a consequence of the smaller Q^2 range, and they would not discriminate between Λ = 10 or Λ = 100 MeV.

iii) Stability of Λ

The EMC results on Λ have been checked against various perturbations :

	$\Delta\Lambda$. MeV
- a change of parametrisation of $F(x,Q_0^2)$ $= 0$ or $x^\alpha \to (a_0 + x^\alpha)$:	0
- apply Fermi motion correction	+ 30
- change $x > 0.2$ to $x > 0.3$ H_2	+ 10
- change $x > 0.2$ to $x > 0.3$ Fe	- 45
- change $R = 0$ to $R = 0.2$ H_2	- 85
- change $R = 0$ to $R = 0.2$ Fe	- 70
- change x to $\zeta = \dfrac{2x}{1+\sqrt{1+4M^2x^2/Q^2}}$ $M = 0.938$	+ 10

(no change for BCDMS)

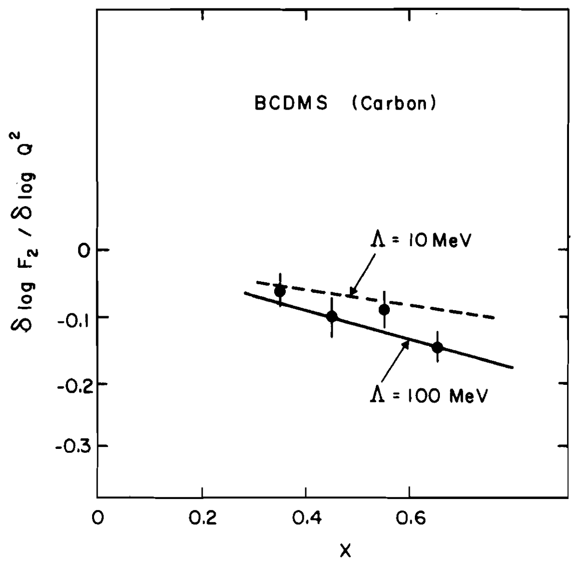

Fig. 15 – Logarithmic slopes of $F_2^{\mu C}$ (BCDMS) : δ Log F_2/δ Log Q^2 as a function of x for Q^2 > 10 GeV^2.

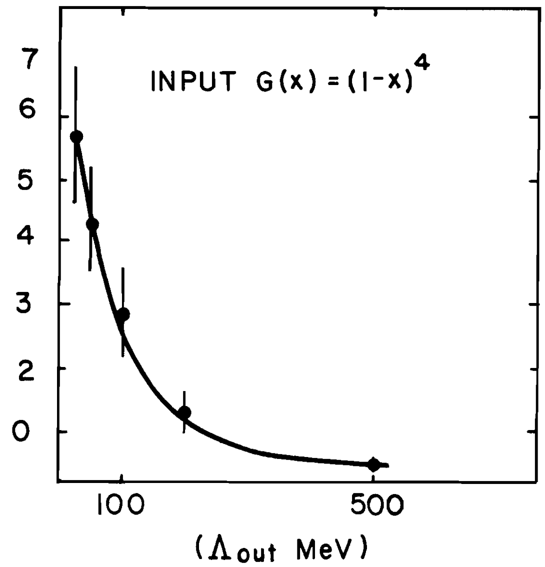

Fig. 16 – Correlation between the value of Λ and the exponent of the gluon distribution, extracted from an Altarelli-Parisi fit.

To observe the effect of a charge in Q^2 cut, the easiest is to compare with the same analysis carried on the F_2 data of the SLAC-MIT group [2] in ep, e D_2 scattering. For x > 0.3, $Q^2 \geqslant 2$ GeV2, we find

$$\Lambda = 310 \text{ MeV } (H_2) \quad \chi^2/N = 3$$
$$\Lambda = 273 \text{ MeV } (D_2) \quad \chi^2/N = 3.6$$

such bad values of χ^2/N indicate that correction terms are needed to lowest order QCD, and that the rise of Λ is probably due to mass dependent contributions.

iv) Low x analysis (x < 0.3)

Once Λ has been found from the high x analysis, the low x measurements of EMC can be used to find an overall description of F_2 in the full x range. A gluon distribution is chosen : $G^2(x,Q_0^2) = g_o\ (1 - x)^5$ at $Q_0^2 = 30$ GeV^2 and g_o is normalised so as to satisfy the momentum some rule

$$\int_0^1 (F_2 + x\, G(x))\, dx = 1$$

Then the hydrogen data is parametrised as

$$F_2^p = \frac{1}{2}\,(F_2^p + F_2^n) + \frac{1}{2}\,(F_2^p - F_2^n)$$

$$\frac{1}{2}\,(F_2^p + F_2^n) = A\, x^{\alpha}\, (1-x)^{\beta}\, (1-\gamma x)$$

$\frac{1}{2}\,(F_2^p - F_2^n)$ is taken from the SLAC-MIT measurements.

It is seen on figure 11 that the whole x domain is easily described with

3 parameters (A, α, β)
1 fixed value of Λ = 110 MeV
1 largely arbitrary function $G(x, Q_0^2)$.

A similar analysis has been carried for the iron data and is also shown on figure 6.

This smooth extension to low x shows that we are not too far from a detailed understanding of scale breaking effects. A hidden difficulty is the correlation investigated by D'Agostini and Payre between the power n on the gluon distribution $G(x,Q_0^2) = \sigma_o(1-x)^n$ and the value of Λ [21], as displayed on figure 16, when an Altarelli Parisi fit is performed over the full x range of the EMC data.

A real non singlet measurement $F_2^p - F_2^n$ is needed to obtain decoupled equations for the determination of Λ and G(x). New data on μ D_2 scattering will soon be available from the EMC collaboration which contributes already with the preliminary measurement of σ_n/σ_p in μ scattering given in figure 17.

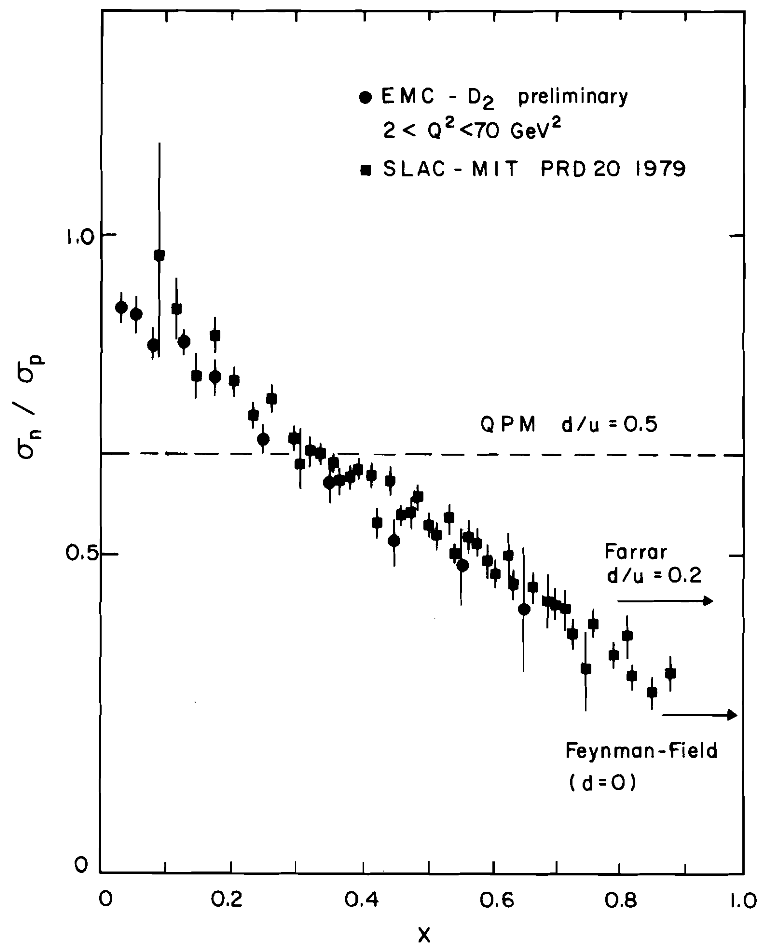

Fig. 17 - x dependence of the ratio σn/σp of deep inelastic cross sections on neutron and proton for SLAC-MIT [2] (Q^2 > 1 GeV^2) and EMC (Q^2 < 70 GeV^2).

V. NEUTRAL CURRENTS IN MUON SCATTERING

No physics result has yet been obtained in this field by the CERN muon experiments. Data was taken by BCDMS with μ^+ and μ^- beams to measure the charge asymmetry in deep inelastic scattering on carbon, which is a superposition of weak effects $B_W = \frac{\sigma^+(Q^2) - \sigma^-(Q^2)}{\sigma^+(Q^2) + \sigma^-(Q^2)} = 1.6\ 10^{-4}\ Q^2\ \text{GeV}^2$ from M. Klein [22] and second order radiative corrections. $4\ 10^6$ deep inelastic events have been registered at 200 and 120 GeV incident energies.

10^6 events already available give a feeling for the present level of systematics on flux monitoring and field reproducibility on figure 18. The same figure shows low Q^2 data from the EMC collaboration without any specific attempts to correct for small systematics or radiative effects.

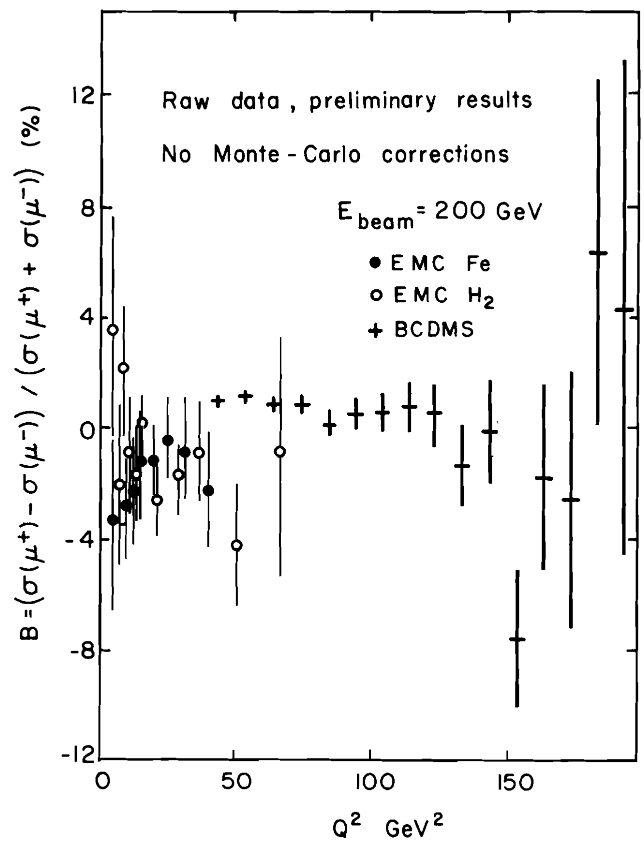

Fig. 18 - Raw results on charge asymmetry

$$B = \frac{(\sigma^{\mu+}(Q^2) - \sigma^{\mu-}(Q^2))}{(\sigma^{\mu+}(Q^2) + \sigma^{\mu-}(Q^2))}$$

in EMC and BCDMS experiments.

VI. CONCLUSIONS

After correcting for Fermi motion, the CERN muon experiments agree to within 3 - 4 % when different energies are combined. The agreement with ν data from CDHS is also excellent.

There is a discrepancy of 10 % in normalisation between μ experiments and e H_2 or e D_2 scattering, which may be partially correlated with uncertainties on R.

The values of Λ found range from 10 to 130 MeV, and within systematics up to 250 MeV, but the experiment with the wider Q^2 range (EMC) definitely favours values around 100 MeV, which is a reasonable 1981 guess.

A quantitative analysis of the gluon structure function is still in progress, and will be constrained by the new D_2 data, helping to reduce the range of Λ from 10 - 250 MeV to ...

Acknowledgements

I would like to thank all colleagues from the BCDHS and EMC experiments, and in particular J. Carr, M. Rith, P. Payre and Y. Sacquin for clarifying discussions and help in preparing these notes. I have also benefitted from lecture notes prepared by H. Wahlen for the SLAC Summer Institute.

REFERENCES

[1] E.D. Bloom et al., Phys. Rev. Letters 23 (1969) 930.
M. Breidenback et al., Phys. Rev. Letters 23 (1969) 935.
G. Miller et al., Phys. Rev. D5 (1972) 528.
J.S. Poucher et al., Phys. Rev. Letters 32 (1974) 118.
S. Stein et al., Phys. Rev. D12 (1975) 1884.

[2] A. Bodek et al., Phys. Rev. D20 (1979) 1471.

[3] BCDMS Collaboration : Bologna (Istituto di Fisica), CERN, Dubna (JINR), Munich (Section Physik der Universität), Saclay (C.E.N.).
D. Bollini et al., Phys. Letters 104B (1981) 403.

[4] European Muon Collaboration : CERN, DESY (Hamburg), Freiburg, Kiel, Lancaster, LAPP (Annecy), Liverpool, Oxford, Rutherford, Sheffield, Torino, Wuppertal.

[5] E.M.C. ; O.C. Allkofer et al., Nuclear Instr. Met. 179 (1981) 445.

[6] SLAC-MIT : (Cf [1], [2]).
CHIO : Gordon et al., Phys. Rev. Letters 41 (1978) 615.
CMP : C. Chang et al., Phys. Rev. Letters 35 (1975) 901.
BFP : A.R. Clark et al., Int. Symp. Lept. Phot. Fermilab 1979.

[7] C. Richard Serre, CERN 71-18 (1971).

[8] L.W. Mo and Y.S. Tsai, Rev. Mod. Phys. 41 (1969) 205.

[9] A.A. Akhundov et al., Dubna preprint 10744 (1976).

[10] EMC : J.J. Aubert et al., Z. Phys. C, Particles and Fields 10 (1981) 93.

[11] C. Chahine, Collège de France preprint LPC 80-03.

[12] I.A. Savine and J. Zacek, JINR Dubna report E1 12502 (1979).

[13] A. Bodek and J.L. Ritchie, Phys. Rev. D23 (1981) 1070.

[14] A.R. Clark et al., Phys. Rev. Letters 45 (1980) 682.

[15] C.G. Callan and D.J. Gross, Phys. Rev. Letters 22 (1969) 156.

[16] H. Wahl in 16ème Rencontres de Moriond, Les Arcs (1981).

[17] L.F. Abbot, W.B. Atwood, R.M. Barnett, Phys. Rev. D22 (1980) 582.

[18] A. Gonzales-Arroyo, C. Lopez, F.J. YNDURAIN, Nuclear Phys. B153 (1979) 161 and Nuclear Phys. B159 (1979) 512.

[19] G. Altarelli and G. Parisi, Nuclear Phys. B126 (1977) 298.

[20] S.J. Brodsky and G. Farrar, Phys. Rev. Letters 31 (1973) 1153.
R. Blankenbecler, S.J. Brodsky, J.F. Gunion, Phys. Rev. Letters 42B (1974) 461.
V.A. Matveev, R.M. Muradyan, A.N. Tavkhalidze, Lett. Nuovo Cimento 7 (1973) 719
F.E. Close, Rep; Prog. Phys. 42 (1979) 1285.

[21] G. D'Agostini and P. Payre, Private communication.

[22] E. Derman, Phys. Rev. D19 (1979) 133.
M. Klein, Ecole de physique de Kupari (1979).

Discussion

H. Wahlen, Gesamthochschule Wuppertal: I have a question about your comparison with the SLAC data. You said this comparison is insensitive to R. I think this is only true as far as you look at the muon data. The SLAC data, I think, are well dependent on R in such a comparison, so my question is what did you assume for R in the SLAC data?

G. Smajda: The SLAC data have a value of R which is published and which is rather accurate. I separated R in the analysis of F_2, so I did not play with the value of R of the SLAC data. I only changed R of the muon data from 0 to .2. In fact, it is very hard for an outsider to change R in the SLAC data because each point would have to be assigned an energy and I would not know how to do that.

O. Nachtmann, Univ. of Heidelberg: I would like to comment on your comparison of Λ extracted from the SLAC-MIT data and from the EMC data. From the theoretical point of view you would expect a difference in the values of Λ, just because you are going from three effective flavors at SLAC to four or five effective flavors at EMC. This will change your Λ by a factor of two.

G. Smajda: Personally, I do not know the rule for counting flavors. I think, this was one of the questions put here. Are the E's a function of x and q^2?

O. Nachtmann: Well, it should really be only a function of q^2. If you have low q^2-values like at SLAC then you should use three effective flavors, at higher values of q^2 you should probably use five already. That will change your effective Λ, essentially you have neglected all quark mass effects in your analysis, which is certainly not correct.

G. Smajda: I agree, that is exactly the point. If the value of Λ is different, it is an indication of mass terms. But as far as the number of flavors is concerned, I do not know how to treat them, in other words what should be the rule. But it is very likely, that the difference is due to mass terms.